NASA Technical Memorandum 89160

RETRIEVAL OF UPPER ATMOSPHERE PRESSURE-TEMPERATURE PROFILES

FROM HIGH RESOLUTION SOLAR OCCULTATION SPECTRA

C. P. Rinsland, J. M. Russell III, J. H. Park,
and J. Namkung

MAY 1987

National Aeronautics and
Space Administration

Langley Research Center
Hampton, Virginia 23665

Summary

The technique of nonlinear least squares spectral curve fitting has been used to retrieve pressure-temperature profiles over the 18- to 75-km altitude range from 0.01-cm^{-1} resolution infrared solar absorption spectra recorded by the ATMOS (Atmospheric Trace Molecule Spectroscopy) Fourier transform spectrometer during the Spacelab 3 shuttle mission in April-May 1985. Preliminary results obtained for four occultation events at 25.6°-30.5°N. and one occultation event at 49.0°S. are compared to correlative measurements.

I. Introduction

Accurate quantitative interpretation of infrared spectra recorded with a limb-viewing instrument requires knowledge of the vertical pressure-temperature profile. This information is often determined from separate rocketsonde or radiosonde measurements or is adopted from climatological data. Because in some cases this information may be incomplete or inaccurate, particularly for a satellite experiment with global coverage, methods are needed to infer accurate pressure-temperature profiles directly from the measured spectra. This approach also has the advantage of avoiding systematic errors which might result from uncertainties in the geometric parameters (instrument altitude, pointing angle, etc.). Toth [1977] used measurements of integrated absorption by high-J lines in the R branch of the 4.3-μm ν_3 band of $^{12}C^{16}O_2$ to retrieve a stratospheric temperature profile from high resolution spectra recorded by a balloon-borne interferometer. Park et al. [1980] and Park [1982] analyzed the same set of near-infrared spectra to obtain both pressure and temperature from integrated absorption measurements of CO_2 lines having different lower state energies. Rinsland et al. [1983a] used the technique of nonlinear least squares spectral curve fitting to derive a stratospheric temperature profile from measurements of the 10.4-μm band of CO_2 in a different series of balloon-borne solar spectra. Techniques for retrieving pressure and temperature from high resolution spectra need to be refined, validated, and applied in additional regions of the infrared. It is particularly important to be able to retrieve pressure and temperature from spectra which also contain atmospheric molecules of importance in understanding upper atmosphere chemistry and dynamics.

The flight of the ATMOS (Atmospheric Trace Molecule Spectroscopy) Fourier transform spectrometer aboard the Spacelab 3 shuttle mission from April 30 to May 6, 1985 [Farmer and Raper, 1986] has provided such an opportunity. Prior to launch, four research groups (JPL, Ohio State University, Oxford University, and NASA Langley) were given the assignment of developing pressure-temperature retrieval algorithms which could be used for operational processing of ATMOS data. The results obtained for Spacelab 3 by the various groups were to be compared with each other and with correlative pressure-temperature data to validate procedures, provide pressure-temperature profiles for the minor and trace gas profile analyses, and aid in selecting the best approach for retrieving pressure and temperature from spectra recorded during future ATMOS missions. In this report, we describe the pressure-temperature retrieval algorithm developed by the NASA Langley group. It was developed on the Langley CDC computer system and has been transferred to the JPL ATMOS Prime computer for on-line, rapid processing of ATMOS spectra. We present for five Spacelab 3 occultations a comparison between pressure-temperature profiles retrieved with our algorithm and correlative pressure-temperature profiles deduced from global satellite and radiosonde measurements by the National Meteorological Center (R. Nagatani, private communication, 1985). The methods and retrieved pressure-temperature profiles of the four research groups are discussed and compared in a journal manuscript in preparation.

The authors acknowledge numerous useful discussions with a number of ATMOS science team members and collaborators, especially C. D. Rogers, A. Muggeridge, J. H. Shaw, Bo-Cai Gao, L. Lowes and C. B. Farmer. Research at ST Systems Corporation was supported by the National Aeronautics and Space Administration.

II. ATMOS Experiment Description

The essential elements of the ATMOS instrument are the Sun tracker, telescope, and a double-pass Michelson interferometer. The interferometer uses a moving "cats eye" arrangement to scan the maximum path difference of 47.4 cm and return in about 2.2 seconds, yielding an unapodized resolution of 0.01 cm^{-1}. Four overlapping broadband filters covering altogether 600 to 4700 cm^{-1}, a survey filter (600-4700 cm^{-1}), and a "notch" filter (600-750 cm^{-1} and 2000-2500 cm^{-1}) are mounted on a filter wheel which can be positioned automatically on successive occultation events as designated by the ATMOS science team. The infrared radiation is detected with a HgCdTe element cooled to 77°K using liquid nitrogen. The combination of orbital inclination, spacecraft velocity, and instrument scan time provides double-sided interferograms separated by about 4 km in tangent height. In the lower stratosphere the separation in tangent height is reduced by atmospheric refraction and drift of the suntracker field of view on the solar disk. The instrument operated for almost 2 days, providing about 1500 double-sided interferograms totaling about 9 Gigabytes of data. About 1000 of these scans were recorded under "high Sun" conditions; the remaining 500 scans were recorded under "low Sun" conditions, and these show a wealth of atmospheric absorption features at tangent heights between about 10 and 150 km.

A total of 12 sunset occultations were obtained over the latitude range 25.6°N. to 32.7°N., and 7 sunrise occultations were obtained between 46.7°S. and 49.0°S. The present analysis has utilized the five occultations, four sunsets and one sunrise, recorded with filter #3 (1580-3400 cm^{-1}). The observation date, spacecraft altitude, and the geographical location of the

tangent point are listed for these occultations in Table I (SS=sunset, SR=sunrise). All were obtained with a field of view of 1 milliradian, which corresponds to an altitude range of 2 km at the tangent point.

Each ATMOS spectrum is generated from the inverse Fourier transform of two-sided interferograms and subsequently ratioed at each wavelength to a "high Sun" spectrum to remove solar absorption and emission features. We have analyzed the primary point data (no interpolation), apodized using the strong apodizing function of Norton and Beer [1976]. The signal-to-rms noise of the spectra in the regions ultilized for analysis is typically 150. Below about 25 km, the signal-to-rms noise in the temperature sensing region near 2390 cm^{-1} is reduced by continuous absorption by far wings of strong CO_2 lines and by pressure-induced absorption from the fundamental band of molecular nitrogen [Rinsland et al., 1981].

III. Algorithm and Analysis

As in several previous published studies [Toth, 1977; Park et al., 1980; Park, 1982; Rinsland et al., 1983a], we have chosen to determine atmospheric pressure and temperature from measurements of absorption lines of carbon dioxide. The volume mixing ratio (VMR) has been assumed to be known at all altitudes (adopted values are listed in Table II); the analysis of the spectra proceeds downward to successively lower tangent heights using the "onion-peeling" approach [Russell and Drayson, 1972; Goldman and Saunders, 1979]. Temperature-insensitive lines (lower state energies, E" = 150-500 cm^{-1}) in each spectrum are analyzed to infer the tangent point pressure P with an uncertainty σ_p; temperature-sensitive lines (E" > 1200 cm^{-1}) in each spectrum are analyzed to infer the tangent point temperture T with an uncertainty

σ_T. The measured tangent point pressures and temperatures are adjusted based on their uncertainties using a least squares procedure, as discussed below, to produce a final retrieved pressure-temperature profile in hydrostatic equilibrium.

The analysis begins with ray-tracing calculations performed with the FSCATM program from FASCOD1C [Gallery et al., 1983] assuming the geometric parameters (spacecraft altitude, measurement latitude, and refracted tangent heights) from the Spacelab 3 ephemeris. The 1976 U.S. Standard Atmosphere was adopted as the initial pressure-temperature profile, and with these values, mass paths (in units of pressure times path length) and density-weighted effective pressures and temperatures were calculated for each layer (~1 km thick) and for each ray path.

Pressure and temperature have been determined from each spectrum using the technique of nonlinear least squares spectral curve fitting. This method has proven particularly suitable for spectral analysis because of its complete use of the spectral data, its accuracy in establishing the background level and instrument line shape, and its usefulness in regions of overlapping spectral lines. It also permits the frequency shift of the data and instrument distortion effects such as channeling and baseline (0 percent transmission) shifts to be retrieved in the analysis [cf. Niple, 1980; Hoke and Shaw, 1982; Park, 1983]. The algorithm used in the present analysis is a modified version of the one used previously to retrieve minor and trace gas volume mixing ratio profiles [cf. Rinsland et al., 1982] and a stratospheric temperature profile [Rinsland et al., 1983a].

In addition to solving for the tangent point pressure or temperature, a number of instrumental parameters can be adjusted in fitting each microwindow. To match the backgrounds of the measured and calculated spectra, up to three

adjustable parameters can be included in the analysis. These parameters model the level, the slope, and the curvature of the background using the polynomial expression:

$$I(\nu) = [A_o + A_1(\nu-\nu_o) + A_2(\nu-\nu_o)^2]\tau(\nu) \quad (1)$$

where $I(\nu)$ is the calculated intensity at wavenumber ν; A_o, A_1, and A_2 are the adjustable coefficients for fitting the background; ν_o is a reference wavenumber; and $\tau(\nu)$ is the calculated transmittance at wavenumber ν. A single adjustable parameter is included to account for a wavelength shift between the measured and calculated spectra. If channel spectra are observed in the data, parameters are included to model the amplitude, period, and phase of each component using the expressions of Niple et al. [1980]. The instrument line shape is modeled to account for both intensity and phase errors [cf. Guelachvili, 1981; Park, 1983], including the effects of interferogram smearing [Park, 1982]. Up to 10 parameters can be included to model distortions in the symmetric part of the line shape function using the effective apodization approach [Park, 1983; Park, 1984]. This method has been modified so that all coefficients are adjusted simultaneously after each iteration. Asymmetric line shape distortions are modeled with a single parameter assuming a simple phase error [cf. Niple et al., 1980; Guelachvili, 1981]. The effect of finite field of view [cf. Guelachvili, 1981] is included in the calculation of the line shape.

Typically, the values of only four of the parameters discussed above need to be adjusted to fit the ATMOS spectra to the noise level of the data. These four fitted parameters are the tangent point pressure or temperature, the background level (A_o of Eq. 1 with A_2 and A_3 constrained to zero), the wavelength shift between measured and calculated spectra, and a "straight-line"

effective apodization parameter [Park, 1983]. Phase errors and channel spectra are found to be negligible in all but a few cases. As mentioned previously, at tangent heights below ~25 km, continuous absorption resulting from the pressure-induced fundamental vibration-rotation band of N_2 and the far wings of intense ν_3 band lines of CO_2 affects the shape of the background near 2390 cm^{-1} [Rinsland et al., 1981] where the lines used for temperature sensing are located; this absorption is not simulated in our calculation, and therefore, for these altitudes, it is necessary to include the background coefficients A_1 and A_2 as adjustable parameters to match the background of the measured and calculated spectra.

It is important to note that several assumptions have been made in the analysis. The actual CO_2 volume mixing ratios in the atmosphere may be different than those assumed in the analysis (Table II). There is increasing uncertainty in the CO_2 VMR above 80 km where photolysis is expected to produce a rapid decrease in CO_2 volume mixing ratio with increasing height. To limit the effect of this uncertainty on the results, pressure-temperature values have been retrieved only below 75 km. We assume that the atmosphere is in local thermodynamic equilibrium (LTE) and in hydrostatic equilibrium at all altitudes. The LTE assumption should be a good approximation for altitudes below about 65 km; at higher altitudes, vibrational temperatures may be significantly lower than the kinetic and rotational temperature [cf. Bullitt et al., 1985]. To minimize errors arising from non-LTE effects at high altitudes, we have used only transitions from the ground vibrational state, the population of which is relatively insensitive to temperature. The line shape is assumed to be given by the Voigt profile which results from combined Lorentz collisional and Doppler broadening. The effects of pressure-induced line shifts, sub- or super-Lorentz far-wing line shapes, collisional or Dicke

narrowing, and radial velocity shifts from atmospheric winds are not included in computing the absorption coefficients. The baseline has been assumed to be given by the instrumental zero level. Saturated lines show baseline shifts of up to several percent in the ATMOS spectra, but unfortunately, this shift is found to be wavelength dependent so that it is possible to apply reliable baseline offsets to the data only when there are saturated lines very close to the analysis region. Because of the limited vertical resolution of the measurements ($\simeq$4 km), it is necessary to adopt a model for the variation of the temperature with height over the range of altitudes defined by the tangent points of successive scans. In this work, we have assumed that the change in temperature is linear with altitude over this region. A constant temperature has been assumed above the tangent height of the highest altitude spectrum. The spacing in tangent height of successive spectra is assumed to be correctly represented in the ATMOS Spacelab 3 ephemeris, including the effects of atmospheric refraction on the ray paths and the drift of the Sun tracker, which is caused by differential refraction and differential attenuation across the solar disk during sunrise and sunset. The assumption of the altitude spacing is an important one in applying the constraint of hydrostatic equilibrium to the pressure-temperature profile. Fortunately, there has been considerable work by members of the ATMOS science team (including the authors) to empirically adjust the spacings by fitting CO_2 and N_2 lines in the spectra. Preliminary pressure-temperature profiles retrieved by the four analysis groups were used in these studies. The pressure-temperature profiles reported here are consistent with these empirical spacings. All of the assumptions noted above are under investigation and will be modified as additional refinements are included in the analysis. For example, preliminary retrievals using temperature-insensitive ν_3 band lines indicate that the volume mixing ratio of

CO_2 begins to decrease near 86 km, a lower altitude than adopted in the analysis, and that the falloff of the CO_2 VMR with increasing height is much more rapid than assumed in the reference profile (Table II).

Table III is a listing of the microwindows selected for sensing both temperature and pressure. The temperature-sensitive lines are all R-branch transitions of the intense ν_3 band of $^{12}C^{16}O_2$. The parameters assumed for these lines in the analysis are those from the September 1986 ATMOS line list. Because of the large change in pressure over the range of altitudes considered (~18-75 km), the pressure sensing lines selected for analysis have intensities which vary by over four orders of magnitude. The positions, intensities, and lower state energies of these lines have been taken from analyses of laboratory spectra of CO_2 recorded at 0.01 cm^{-1} resolution by investigators at NASA Langley and William and Mary [Rinsland and Benner, 1984; Rinsland et al., 1980, 1983b, 1984, 1985, 1986, Malathy Devi et al., 1984; Benner and Rinsland, 1985]. These parameters also appear in the September 1986 ATMOS line list. The air-broadened halfwidths for all CO_2 lines are taken from the ATMOS compilation; a $T^{-0.75}$ temperature dependence has been assumed for the variation of the air-broadened halfwidth with temperature.

Each of the microwindows listed in Table III contains between 2 and 19 lines of CO_2. Only one of the microwindows has been used to retrieve the tangent point temperature of each spectrum. The tangent point pressure of each spectrum is obtained from the weighted average of the pressures retrieved from fitting as many as six microwindows. The weight W of each measurement has been calculated as $1/\sigma^2$, where σ is the statistical uncertainty in the pressure from the spectral fitting results. By averaging, the uncertainty in the tangent point pressure retrieved from each spectrum is reduced.

As noted in Table III, several of the microwindows contain minor contamination by solar lines and by atmospheric lines from molecules other than CO_2. To minimize the effect of the atmospheric lines on the retrieval results, their absorption has been included in the calculations and a parameter has been added to solve for the tangent point volume mixing ratio of the contaminant gas. Lines of solar CO occur in many of the microwindows selected for pressure sensing; a few atomic solar lines occur in the microwindows selected for temperature sensing. Because the cancellation of the solar lines is imperfect, particularly at tangent heights below 50 km, the microwindows have been chosen to avoid CO_2 lines which have strong solar features close to their line centers.

The first iteration of the spectral analysis begins by retrieving the vertical pressure profile, assuming the 1976 U.S. Standard Atmosphere temperatures. Because the pressure lines are insensitive to temperature, a fairly good first estimate is obtained. Then, with these retrieved pressures, the temperature-sensitive lines are analyzed to obtain a first estimate of the vertical temperature profile. At this point, the hydrostatic equilibrium constraint is applied to refine the results.

From analysis of N spectra, a total of 2N atmospheric parameters are retrieved: N measurements of tangent point temperatures and N measurements of tangent point pressures. However, the solution is overdetermined to define an atmosphere in hydrostatic equilibrium. For example, N-1 measurements of the temperature gradient between successive spectra and a pressure and temperature at an arbitrary point are sufficient.

Therefore, a program was written to obtain a best-fit hydrostatic atmosphere from the retrieved tangent point pressures and temperatures. As above, each measurement was assigned a weight W given by $1/\sigma^2$, where σ is the

uncertainty from the spectral analysis (typically 5 to 10 percent for the pressures and 1 K for the temperatures). The fitted parameters were the pressure and temperature at the tangent point of the highest altitude spectrum (a constant temperature was assumed above this altitude) and the temperature gradient (degrees Kelvin per km) between the tangent points of the successively lower altitude spectra. The analysis program includes the variation of the acceleration of gravity with latitude and altitude in the calculations.

The best-fit hydrostatic atmosphere and associated mass paths are then used as starting values for the second iteration. Again, the pressure profile is retrieved with the temperature profile fixed. These new pressures and associated uncertainties are used with the temperatures and associated uncertainties from the earlier iteration to refine the estimate of the hydrostatic atmosphere. This procedure is then repeated using the temperature sensing lines, constraining the pressures. At this point, the pressures are found in most cases to differ by <2 percent and the temperature by <1 K from those retrieved after the first iteration.

The analysis is then repeated for a third and final iteration using both the pressure and temperature microwindows. The entire retrieval is automated and runs in the background as a batch job on the ATMOS computer system. All calculations, except the FFT's (Fast Fourier Transforms), are performed in double precision. Array processors are used to calculate the forward and inverse FFT's. Speed is enhanced by storing the absorption coefficients from all layers above the tangent layer. The Drayson [1976] Voigt profile algorithm, which is both fast and accurate [Twitty et al., 1980], is used in the line shape calculations. The CPU time is 4 to 6 hours per occultation, but improvements in the ATMOS computer system are expected to reduce the CPU time significantly.

IV. Results

Typical least-squares fitting results are illustrated in Figures 1 and 2. Figure 1 shows plots for two pressure sensing microwindows; two temperature-sensing microwindows are shown in Figure 2. For each spectrum (all from SS06), the measured intensities are normalized to the highest measured intensity in the microwindow. The residuals (observed minus calculated) are given above each spectrum. In all cases, the standard deviation of the residuals is close to the noise level of the data, indicating satisfactory modeling of the spectral data.

Figures 3 to 7 present a comparison of the retrieved pressure-temperature profiles for SS06, SS09, SS11, SS13, and SR02 and the NMC correlative data for the corresponding geometric locations. The measured temperatures are within the NMC error bars for almost all determinations for the five occultations. However, it is interesting to note that our retrieved temperatures are all warmer than the NMC values near 1 mb, the temperature maximum, for all the sunset occultations. The temperatures retrieved for SS09 between ~3 and ~30 mb are colder than the NMC values. The cause for these discrepancies is unclear. The retrieved profiles for the sunset occultations are all very similar. The profile for SR02 is much different, which is not surprising considering the large difference in the geographic locations of the tangent points of the sunrise and sunset spectra. A large difference between the NMC and Langley temperatures occurs near 0.4 mb in SR02, where the present results indicate a temperature minimum.

Table IV presents a summary of the comparisons between the retrieved and NMC values. The mean temperature difference (NMC minus Langley) is 1.2 K with a standard deviation of 6.0 K. From this result we conclude there is no significant bias between the two sets of temperatures. The NMC uncertainties

increase with altitude and are much larger for the Southern Hemisphere than for the Northern Hemisphere.

V. Summary and Conclusions

A method has been described for retrieving pressure-temperature profiles from the high resolution infrared solar absorption spectra recorded by the ATMOS instrument. The method produces results which are, in most cases, in agreement with correlative measurements within their estimated uncertainties.

The retrieval method is automated, and with the experience gained from analyzing the Spacelab 3 data, it should be possible on future missions to retrieve pressure-temperature profiles for all of the filter #3 occultations within several days of receiving the data. Further work is needed, however, since some of the assumptions noted above may produce systematic errors. Both the effect of non-LTE in CO_2 and the profile of CO_2 in the upper mesosphere and lower thermosphere are being studied. Also, microwindows with well-determined line parameters need to be defined for the other ATMOS filter regions so that pressure-temperature profiles can be retrieved from occultations recorded with these other filters.

Table I

ATMOS Occultations Analyzed for Pressure and Temperature

Occultation	U.T. Date	Spacecraft Altitude (km)	Tangent Point Latitude	Tangent Point Longitude
SR02	4/30/85	363.3	48.9°S	294.4°E
SS06	4/30/85	360.2	30.5°N	291.4
SS09	5/1/85	359.4	26.8°N	15.3
SS11	5/1/85	359.3	26.2°N	329.3
SS13	5/1/85	359.4	25.6°N	283.3

Notes: The altitudes, latitudes, and longitudes are values at a tangent height of about 25 km. The geometric parameters changed slowly during the event. For example, the SS09 occultation values for spacecraft altitude, latitude, and longitude were 359.3 km, 26.5°N, and 15.1°E, respectively, at a tangent height of 14.7 km.

Table II

Assumed CO_2 Volume Mixing Ratio Profile (VMR)

Altitude (km)	CO_2 VMR (ppmv)
130	160
120	160
115	210
110	290
20–105	330
18	332
16	334

Table III

Pressure Sensing Microwindows

SPECTRAL INTERVAL	ALTITUDE RANGE	ISOTOPE	BAND	INTERFERENCE
1909.4-1912.6 cm^{-1}	45 - 55 km	626	11102-00001	H_2O, Solar CO
1913.7-1917.4	45 - 55	626	11102-00001	NO, Solar CO
1932.2-1934.9	30 - 45	626	11102-00001	H_2O, Solar CO
1950.5-1954.0	25 - 30	626	11102-00001	H_2O, Solar CO
2051.8-2053.7	60 - 70	626	11101-00001	Solar CO
2056.4-2058.5	60 - 70	626	11101-00001	Solar CO
2059.5-2063.0	60 - 70	626	11101-00001	CO, Solar CO
2076.0-2079.0	55 - 65	626	11101-00001	CO, Solar CO
2253.5-2257.6	70 - 75	636	00011-00001	Solar CO
2259.3-2263.2	70 - 75	636	00011-00001	Solar CO
2264.8-2268.6	70 - 75	636	00011-00001	Solar CO
2270.1-2273.9	70 - 75	636	00011-00001	Solar CO
2615.5-2617.5	17 - 20	628	20002-00001	-
2619.9-2621.6	20 - 30	628	20002-00001	-

Temperature Sensing Microwindows

SPECTRAL INTERVAL	ALTITUDE RANGE	ROTATIONAL LINES	E"(max)
2380.5-2384.4 cm^{-1}	70 - 75 km	R50 - R58	1334 cm^{-1}
2384.0-2388.1	65 - 70	R58 - R68	1828
2387.0-2389.5	55 - 65	R66 - R72	2047
2389.0-2392.4	50 - 55	R72 - R82	2650
2390.3-2393.8	30 - 50	R76 - R88	3048
2392.0-2393.8	17 - 30	R82 - R88	3048

Notes:
1. All CO_2 lines in the temperature microwindows are rotational transitions in the ν_3 band of $^{12}C^{16}O_2$.
2. Some solar absorption lines occur in the temperature microwindows.
3. E"(max) is the lower state energy of the highest rotational transition within the microwindow.
4. 626 = $^{12}C^{16}O_2$; 636 = $^{13}C^{16}O_2$; 628 = $^{16}O^{12}C^{18}O$.

Table IV

COMPARISON OF NMC AND LANGLEY TEMPERATURE VALUES

PRESSURE (MB)	SS06			SS09			SS11			SS13			SR02		
	NMC	LaRC	ΔT	NMC	LaRc	ΔT	NMC	LaRC	ΔT	NMC	LaRC	ΔT	NMC	LaRC	ΔT
0.4	266	266	0	267	256	+11	266	257	+9	267	257	+10	256	236	+20
1.0	260	269	-9	258	270	-12	261	266	-5	259	263	-4	244	241	+3
2.0	259	264	-5	259	264	-5	261	265	-4	259	263	-4	236	232	+4
5.0	250	243	+7	252	243	+9	251	249	+2	252	250	+2	226	226	0
10.0	235	235	0	239	232	+7	236	232	+4	236	234	+2	220	220	0
30.0	219	219	0	216	211	+5	219	215	+4	218	217	+1	216	215	+1
50.0	211	212	-1	209	209	0	211	215	-4	209	209	0	216	215	+1
70.0	206	208	-2										216	220	-4
MEAN ΔT (NMC-LaRC)			-1.2			+2.1			+0.9			+1.0			+3.1
ST. DEV. OF ΔT			4.6			8.3			5.3			4.7			7.2
# INSIDE NMC UNCERTAINTY			7			3			6			7			7
# OUTSIDE NMC UNCERTAINTY			1			4			1			0			1

References

Benner, D. C., and C. P. Rinsland, Identification and intensities of the "forbidden" $3\nu_2{}^3$ band of $^{12}C^{16}O_2$, J. Mol. Spectrosc., 112, 18-25, 1985.

Bullitt, M. K., P. M. Bakshi, R. H. Picard and R. D. Sharma, Numerical and analytical study of high-resolution limb spectral radiance from non-equilibrium atmospheres, J. Quant. Spectrosc. Radiat. Transfer, 34, 33-53, 1985.

Drayson, S. R., Rapid computation of the Voigt profile, J. Quant. Spectrosc. Radiat. Transfer, 16, 611-614, 1976.

Farmer, C. B., and O. F. Raper, High resolution infrared spectroscopy from space: A preliminary report on the results of the Atmospheric Trace Molecule Spectroscopy (ATMOS) experiment on Spacelab 3," NASA Conference Proceedings, "Spacelab 3 Mission Review," CP-2429, May 1986.

Gallery, W. O., F. X. Kneizys, and S. A. Clough, Air mass computer program for atmospheric transmittance/radiance calculation: FSCATM, Environ. Res. Pap. 828 (AFGL-TR-83-0065), 145 pp., Air Force Geophys. Lab., Bedford, Mass., 1983.

Goldman, A., and R. S. Saunders, Analysis of atmospheric infrared spectra for altitude distribution of atmospheric trace constituents - I. Method of analysis, J. Quant. Spectrosc. Radiat. Transfer, 21, 155-162, 1979.

Guelachvili, G., Distortions in Fourier spectra and diagnosis, in Spectrometric Techniques, Vol. II, ed. G. A. Vanassee, Academic, New York, 1981.

Hoke, M. L., and J. H. Shaw, Analysis of CO_2 bands near 2600 cm^{-1}, Appl. Opt., 21, 929-934, 1982.

Malathy Devi, V., C. P. Rinsland, and D. C. Benner, Absolute intensity measurements of CO_2 bands in the 2395-2680-cm^{-1} region, Appl. Opt., 23, 4067-4075, 1984.

Niple, E., Nonlinear least squares analysis of atmospheric absorption spectra, Appl. Opt., 19, 3481-3490, 1980.

Niple, E., W. G. Mankin, A. Goldman, D. G. Murcray, and F. J. Murcray, Stratospheric NO_2 and H_2O mixing ratio profiles from high resolution infrared solar spectra using nonlinear least squares, Geophys. Res. Lett., 7, 489-492, 1980.

Norton, R. H., and R. Beer, New apodizing functions for Fourier spectroscopy, J. Opt. Soc. Am., 66, 259-264, 1976.

Park, J. H., The effect of interferogram smearing on atmospheric limb sounding by Fourier transform spectroscopy, Appl. Opt., 21, 1356-1366, 1982.

Park, J. H., Analysis method for Fourier transform spectroscopy, Appl. Opt., 22, 835-849, 1983.

Park, J. H., Analysis and application of Fourier transform spectroscopy in atmospheric remote sensing, Appl. Opt., 23, 2604-2613, 1984.

Park, J. H., J. M. Russell III, and M. A. H. Smith, Solar occultation sounding of pressure and temperature using narrow band radiometer, Appl. Opt., 19, 2132-2139, 1980.

Rinsland, C. P., and D. C. Benner, Absolute intensities of spectral lines in carbon dioxide bands near 2050 cm^{-1}, Appl. Opt., 23, 4523-4528, 1984.

Rinsland, C. P., A. Baldacci, and K. Narahari Rao, Strengths of $^{13}C^{16}O_2$ lines at 4.3 μm, J. Mol. Spectrosc., 81, 256-261, 1980.

Rinsland, C. P., M. A. H. Smith, J. M. Russell III, J. H. Park, and C. B. Farmer, Stratospheric measurements of continuous absorption near 2400 cm^{-1}, Appl. Opt., 20, 4167-4171, 1981.

Rinsland, C. P., A. Goldman, F. J. Murcray, D. G. Murcray, M. A. H. Smith, R. K. Seals, Jr., J. C. Larsen, and P. L. Rinsland, Stratospheric N_2O mixing ratio profile from high-resolution balloon-borne solar absorption spectra and laboratory spectra near 1880 cm^{-1}, Appl. Opt., 21, 4351-4355, 1982.

Rinsland, C. P., A. Goldman, F. J. Murcray, D. G. Murcray, M. A. H. Smith, R. K. Seals, Jr., J. C. Larsen, and P. L. Rinsland, Stratospheric temperature profile from balloon-borne measurements of the 10.4-μm band of CO_2, J. Quant. Spectrosc. Radiat. Transfer, 30, 327-334, 1983a.

Rinsland, C. P., D. C. Benner, D. J. Richardson, and R. A. Toth, Absolute intensity measurements of the $(11^10)_{II} \leftarrow 00^00$ band of $^{12}C^{16}O_2$ at 5.2 μm, Appl. Opt., 22, 3805-3809, 1983b.

Rinsland, C. P., D. C. Benner, V. Malathy Devi, P. S. Ferry, C. H. Sutton, and D. J. Richardson, Atlas of high resolution infrared spectra of carbon dioxide, Appl. Opt., 23, 2051-2052, 1984.

Rinsland, C. P., D. C. Benner, and V. Malathy Devi, Measurements of absolute line intensities in carbon dioxide bands near 5.2 μm, Appl. Opt., 24, 1644-1650, 1985.

Rinsland, C. P., D. C. Benner, and V. Malathy Devi, Absolute line intensities in CO_2 bands near 4.8 μm, Appl. Opt., 25, 1204-1214, 1986.

Russell, J. M. III, and S. R. Drayson, The inference of atmospheric ozone using satellite horizon measurements in the 1042 cm^{-1} band, J. Atmos. Sci., 29, 376-390, 1972.

Toth, R. A., Temperature sounding from the absorption spectrum of CO_2 at 4.3 μm, Appl. Opt., 16, 2661-2668, 1977.

Twitty, J. T., P. L. Rarig, and R. E. Thompson, A comparison of fast codes for the evaluation of the Voigt profile function, J. Quant. Spectrosc. Radiat. Transfer, 24, 529-532, 1980.

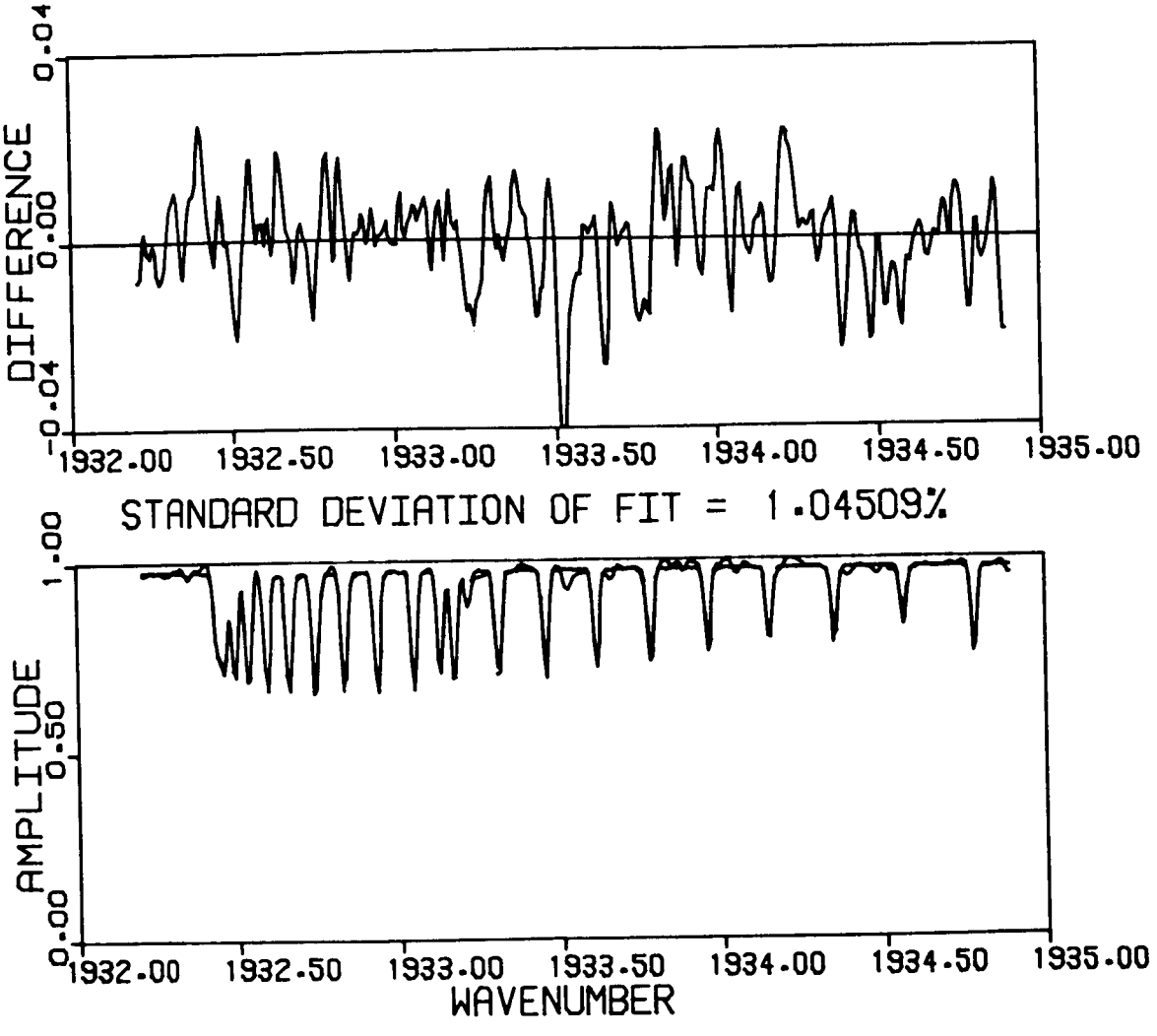

Fig. 1a. Least squares fitting results for an interval containing a pressure-sensitive Q branch of carbon dioxide. The tangent height for this scan (R50430230722) is 38.7 km.

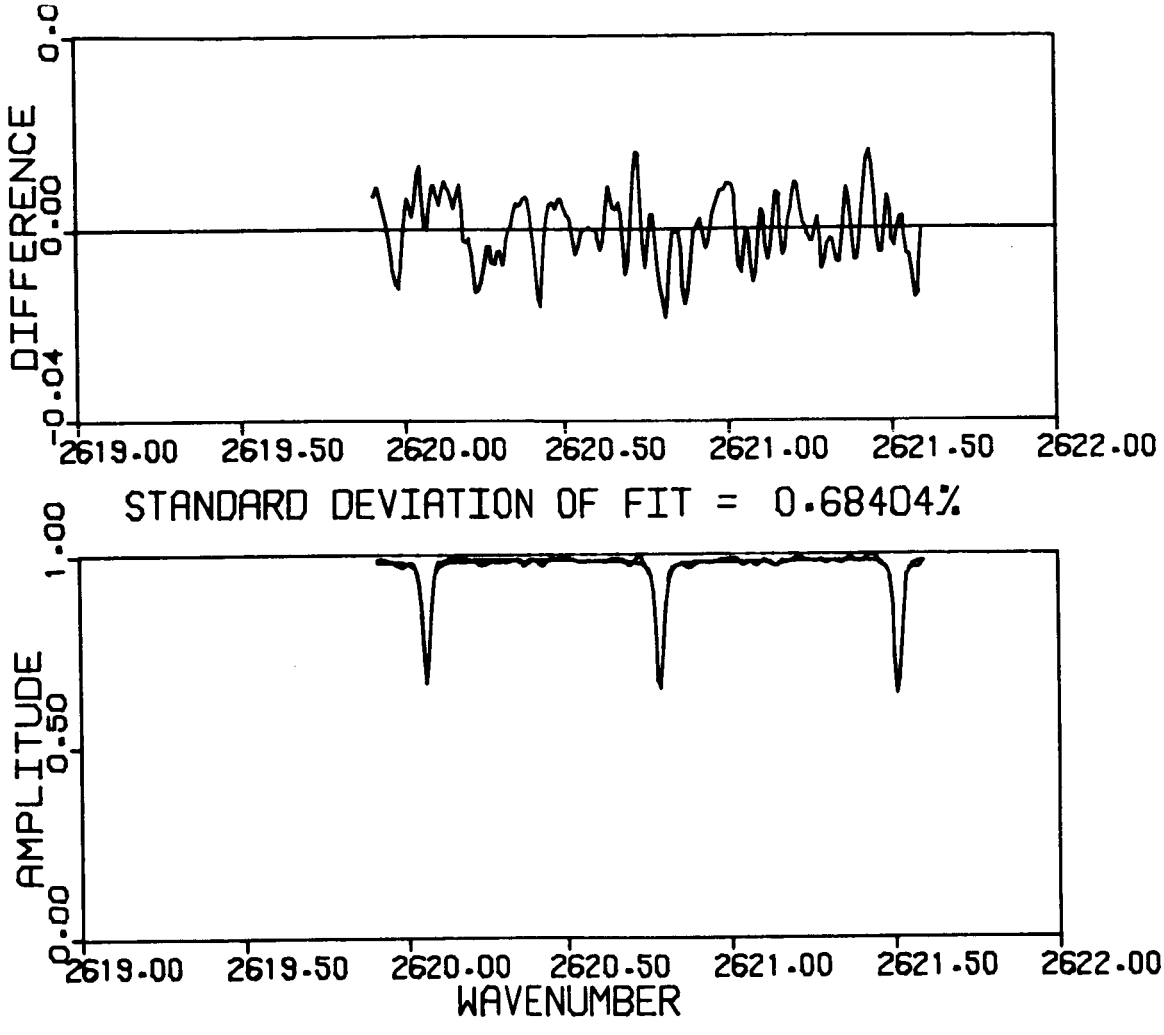

Fig. 1b. Least-squares fitting results in an interval containing 3 pressure-sensitive lines of carbon dioxide. The tangent height of this scan (R50430230733) is 20.5 km.

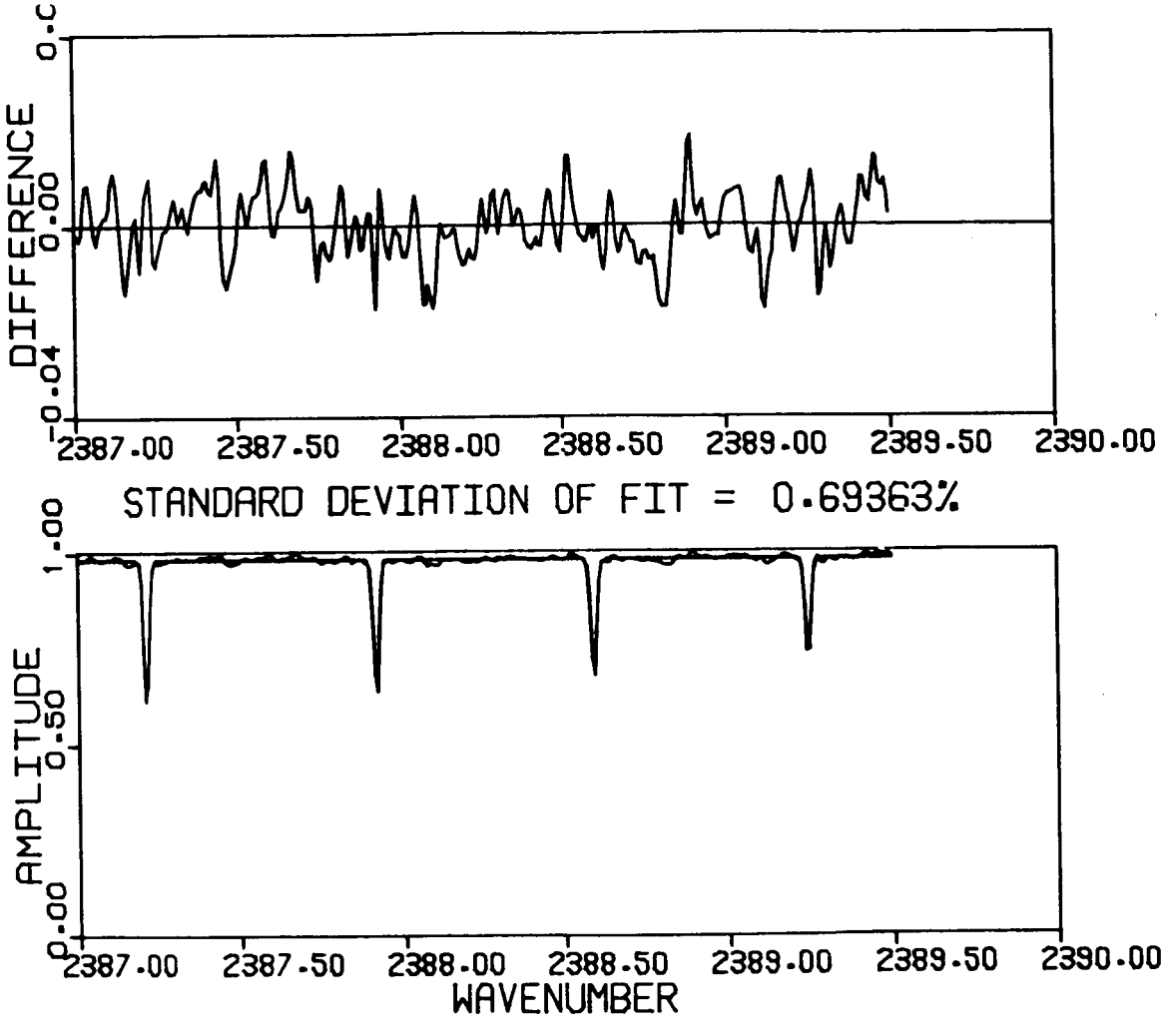

Fig. 2a. Least-squares fitting results in one of the temperature-sensing microwindows. The tangent height for this scan (R50430230711) is 60.4 km.

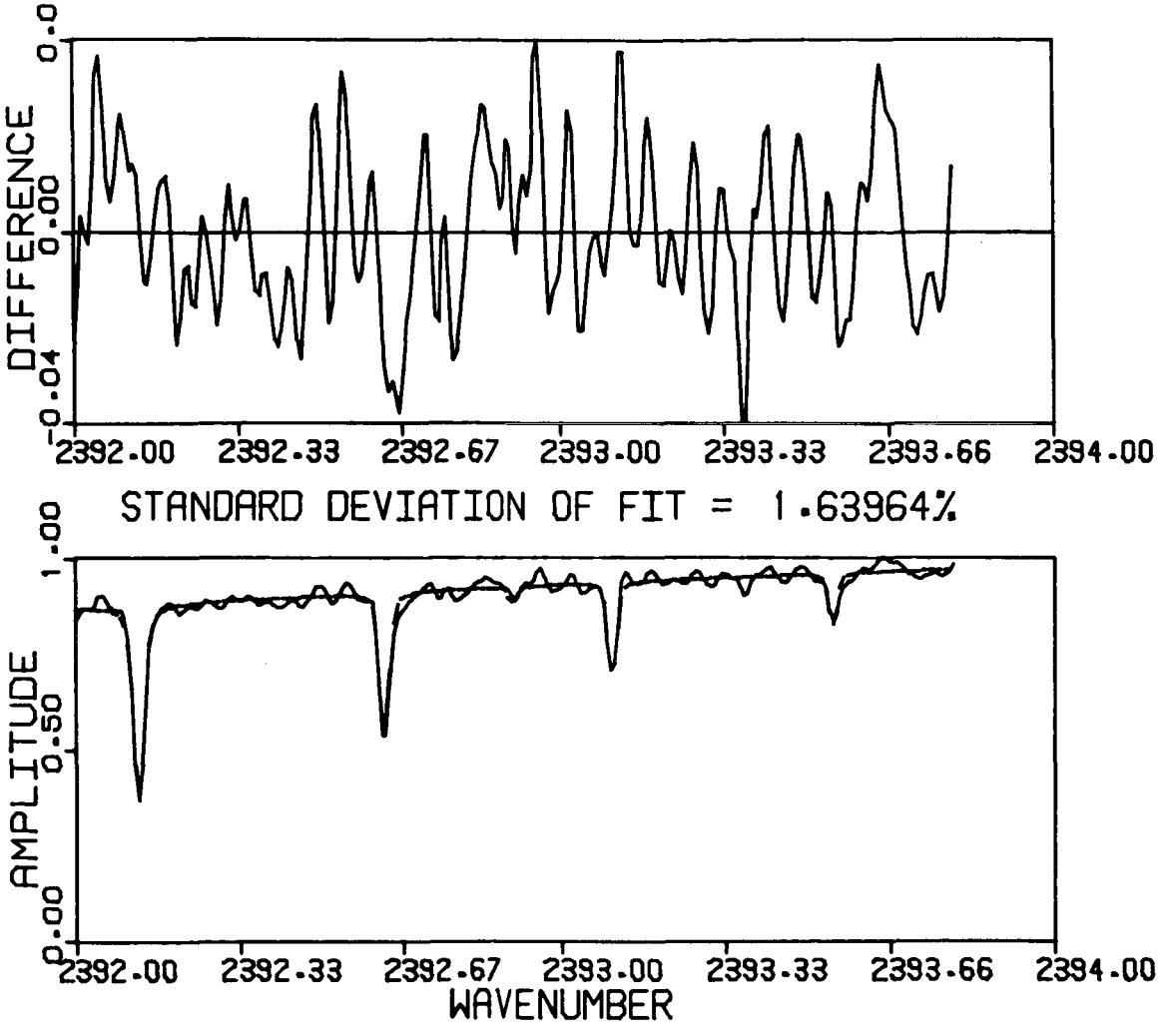

Fig. 2b. Least-squares fitting results in one of the temperature-sensing microwindows. The tangent height for this scan (R50430230735) is 17.7 km. The slope in the background in this region is caused by continuous absorption by molecular nitrogen and far wings of intense CO_2 lines.

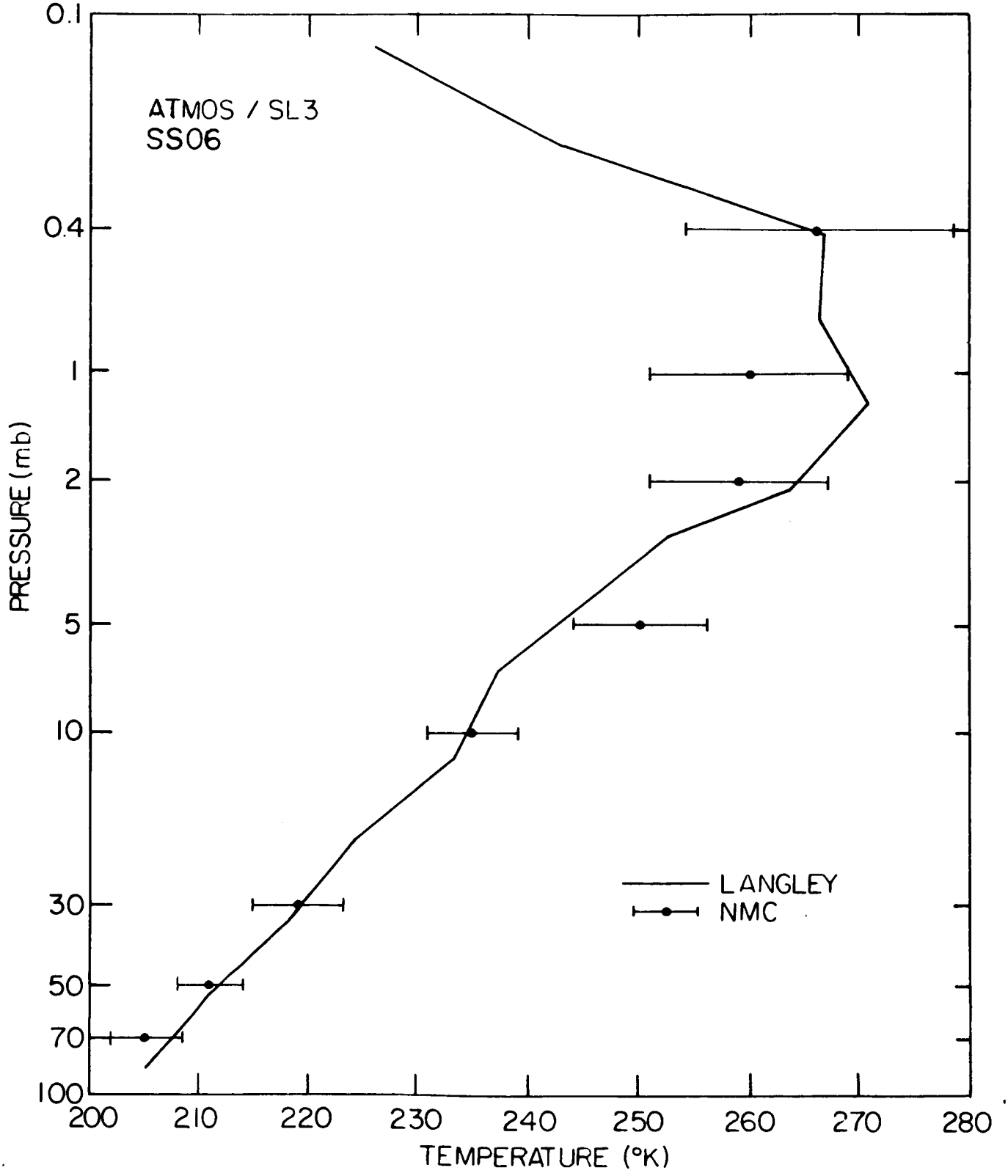

Fig. 3. Comparison of pressure-temperature results obtained with the present algorithm and NMC values for the SS06 filter 3 occultation.

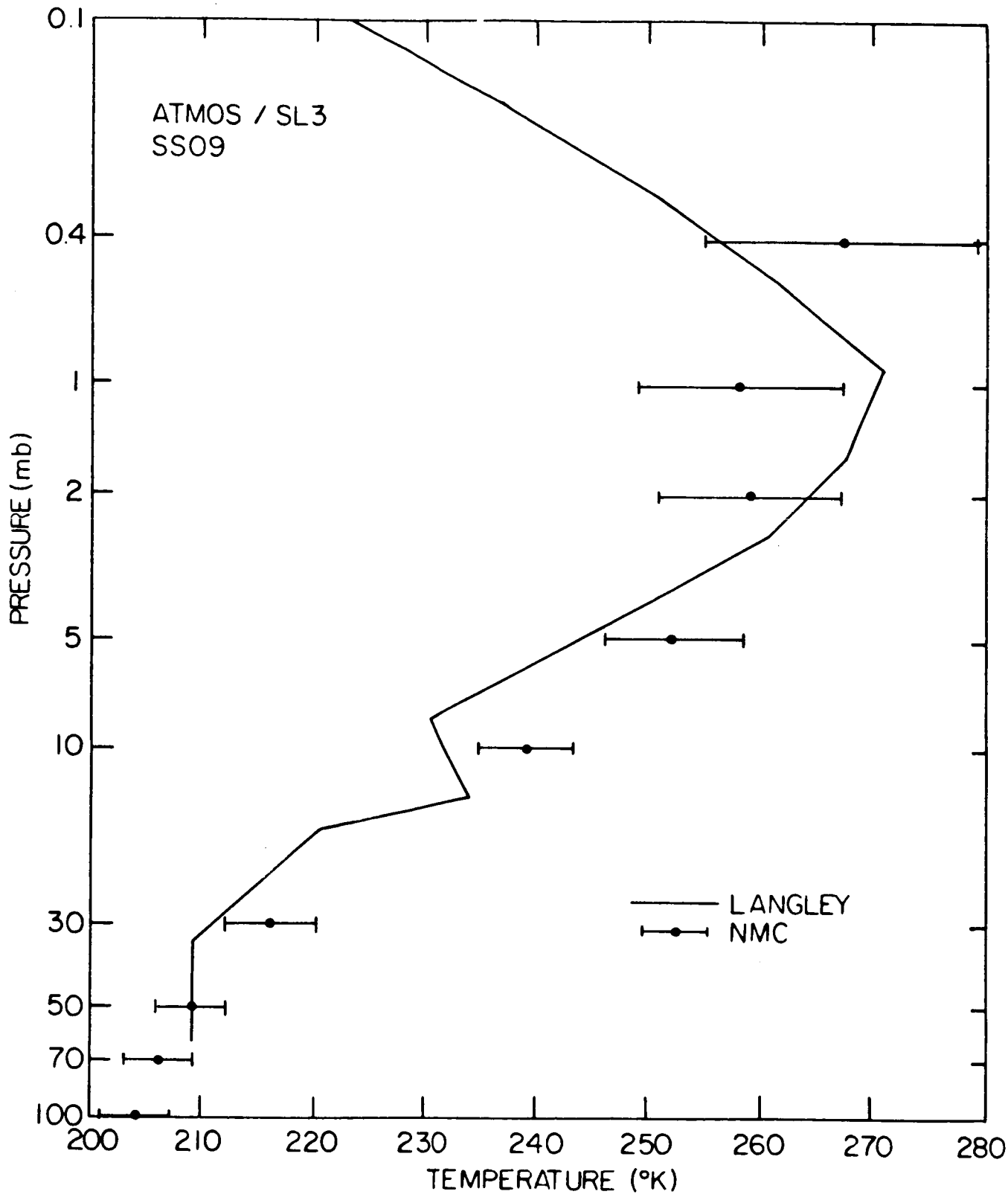

Fig. 4. Comparison of pressure-temperature results obtained with the present algorithm and NMC values for the occultation SS09.

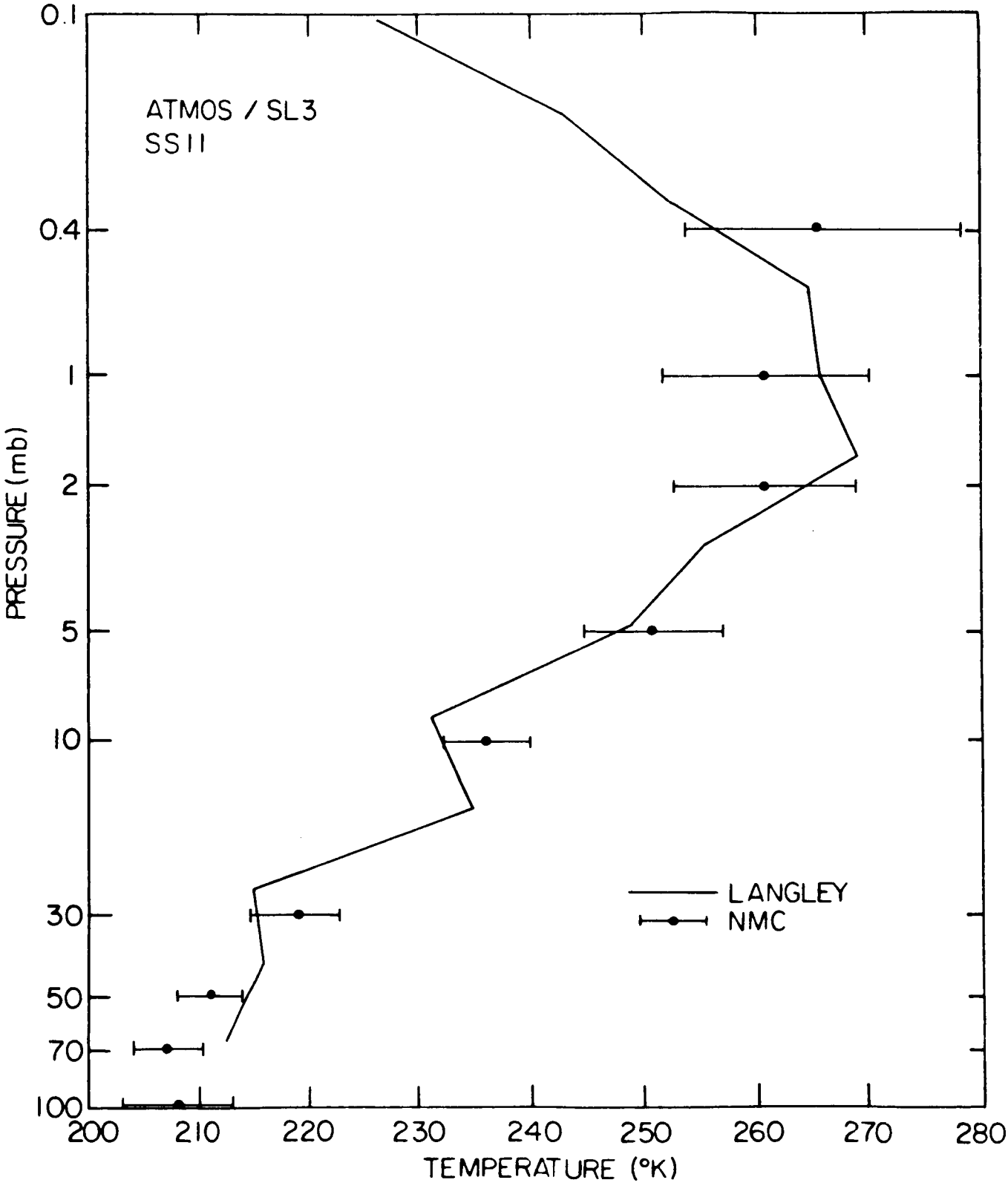

Fig. 5. Comparison of pressure-temperature results obtained with the present algorithm and NMC values for the occultation SS11.

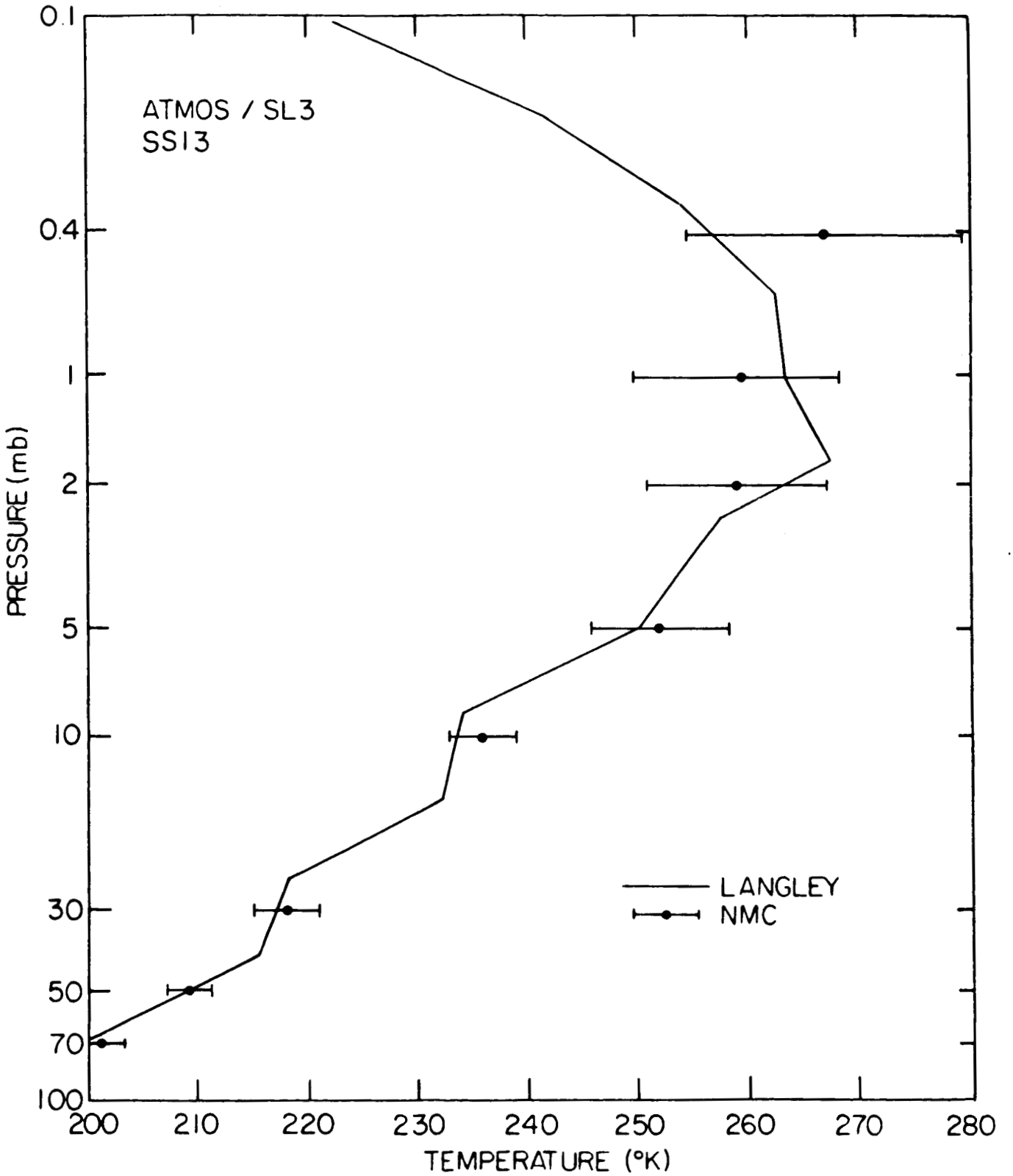

Fig. 6. Comparison of pressure-temperature results obtained with the present algorithm and NMC values for the occultation SS13.

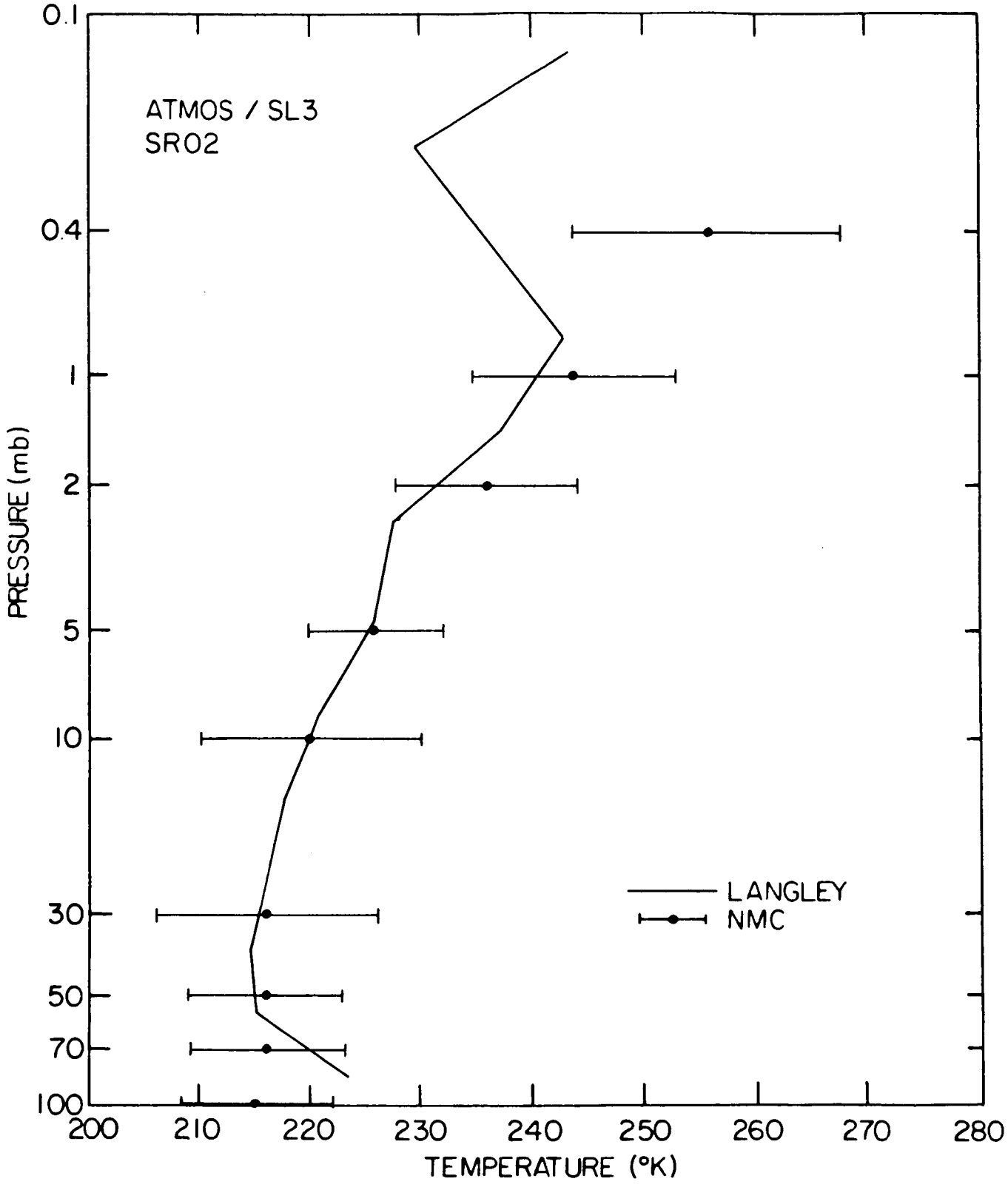

Fig. 7. Comparison of pressure-temperature results obtained with the present algorithm and NMC values for the occultation SR02.

Standard Bibliographic Page

1. Report No.	2. Government Accession No.	3. Recipient's Catalog No.
NASA TM-89160		

4. Title and Subtitle	5. Report Date
Retrieval of Upper Atmosphere Pressure-Temperature Profiles from High Resolution Solar Occultation Spectra	May 1987
	6. Performing Organization Code
7. Author(s)	8. Performing Organization Report No.
C. P. Rinsland, J. M. Russell III, J. H. Park, and J. Namkung*	
9. Performing Organization Name and Address	10. Work Unit No.
	618-21-00-01
NASA Langley Research Center Hampton, VA 23665-5225	11. Contract or Grant No.
12. Sponsoring Agency Name and Address	13. Type of Report and Period Covered
National Aeronautics and Space Administration Washington, DC 20546	Technical Memorandum
	14. Sponsoring Agency Code

15. Supplementary Notes

*ST Systems Corporation
17 Research Drive
Hampton, VA 23666

16. Abstract

Pressure-temperature profiles over the 18-75 km altitude range have been retrieved from 0.01 cm^{-1} resolution infrared solar absorption spectra recorded with the ATMOS (Atmospheric Trace Molecule Spectroscopy) Fourier transform spectrometer operating in the solar occultation mode during the Spacelab 3 shuttle mission (April 30-May 1, 1985). The analysis method is described and preliminary results deduced for five occultation events are compared to correlative pressure-temperature measurements.

17. Key Words (Suggested by Authors(s))	18. Distribution Statement
Remote sensing Atmospheric optics Infrared spectra Atmospheric gases	Unclassified--Unlimited Subject category: 46

19. Security Classif.(of this report)	20. Security Classif.(of this page)	21. No. of Pages	22. Price
Unclassified	Unclassified	33	A03

For sale by the National Technical Information Service, Springfield, Virginia 22161